Power LED junction temperature readout circuit based on an off-the-shelf LED driver

Demetrio Iero[1,2], Massimo Merenda[1,2], Sonia Polimeni[1], Riccardo Carotenuto[1], Fortunato Pezzimenti[1], Sandro Rao[1], Francesco G. Della Corte[1,2]
[1] DIIES, Mediterranea University of Reggio Calabria, Reggio Calabria 89122, Italy
[2] HWA s.r.l.-Spin Off of the Mediterranea University of Reggio Calabria, Reggio Calabria, 89126 Italy
demetrio.iero@unirc.it

***Abstract*—A circuit is presented for the on-line measurement of the junction temperature (T_J) of power LEDs. The circuit is integrated with, and makes use of, an off-the-shelf LED driver, so that the proposed architecture can be easily made compatible with existing high-end luminaire platforms. The measurement technique, based on the linear junction voltage *vs.* temperature relationship, shows good precision and repeatability among devices with the same part number, with an absolute error below 3 °C.**

***Keywords*—temperature sensors; power LED; junction temperature**

I. INTRODUCTION

Light emitting diodes (LEDs) are the most efficient and durable light sources. Their efficiency and service life outclass other light sources as incandescent or fluorescent bulbs the place of which they are rapidly taking over. However, LEDs can safely operate only at a limited maximum temperature, after which their expected service life is drastically reduced and the emitted light is irreversibly degraded as well [1]–[4]. It is therefore necessary to keep the operating temperature under control.

Temperature can be measured with different techniques [5]–[9], but some of these techniques [6]–[8] are of difficult implementation. The device junction temperature (T_J) can be estimated by using the thermal data provided by the manufactured, such as the die-to-case thermal resistance, and measuring the package (or heat-sink) temperature and the dissipated power [10], [11]. However, this approach gives only an approximative value of T_J and it does not allow to detect fast temperature variations. Other techniques to measure the LED junction temperature leverage on the dependence of some electrical parameters from the temperature, *e.g.* the reverse saturation current I_0 [12] or the forward voltage drop V_F [13], [14].

The high linearity of the V_F vs. T_J relationship in a proper current range has already been demonstrated in a previous work [15]. There, obtained results have been used to measure directly the LED temperature, without the use of external temperature sensors, with a simple pre-calibration procedure to determine the coefficients of the linear relationship.

In this work, the same method has been applied to measure the temperature of the LEDs in a string using a commercial off-the-shelf power LED driver to demonstrate the application of the technique in a practical circuit, easily deployable in high-end luminaires. The driver, which is able to drive several LEDs in series, is paired with a microcontroller that sets the driver working mode and performs the temperature measurement at regular intervals in such a way that it does not affect the light perceived by the human eye.

The paper is organized as follows: Section II describes the junction temperature measurement theory and the used technique; Section III describes the LED driving and measurement circuit; Section IV and V present the experimental results and conclusions, respectively.

II. LED JUNCTION TEMPERATURE MEASUREMENT

As for any other solid-state junction device, there exists a relationship between the voltage across a junction and the junction temperature, allowing an indirect temperature measurement. The electrical characteristic of a LED is in fact similar to that of a standard diode and it can be expressed with the equation:

$$I_F = I_0\left(e^{\frac{qV_F}{nkT}} - 1\right), \tag{1}$$

where I_F is the LED current, V_F is the LED forward voltage, n is the ideality factor, I_0 is the saturation current, k is the Boltzmann constant, T is the junction temperature, and q is the electron charge. Neglecting the unity, the relationship can be simplified as:

$$V_F = n\frac{kT}{q}(lnI_F - lnI_0). \tag{2}$$

The apparent linear dependence of V_F on temperature of (2) is unfortunately compromised by the temperature dependence of I_0 [16], [17], *i.e.*

$$I_0 = C\,T^{\alpha}\,e^{-\frac{E_g}{kT}}, \tag{3}$$

where C and α are constants, and E_g is the energy bandgap calculated at 0 K. Therefore, (2) can be written as:

$$V_F = n\frac{kT}{q}[lnI_F - lnC - \alpha\, lnT] + \frac{n}{q}E_g. \tag{4}$$

This equation shows a nearly linear dependence of the voltage from the temperature as the lnT term changes by a small amount in the typical operating temperature range for LEDs as shown in [18]–[22]. Consequently, the previous expression can be approximated as:

$$V_F = S \cdot T + Q, \tag{5}$$

where S and Q are current-dependent coefficients, extracted for a certain device model. From (5), T_J can be calculated by simply measuring the voltage across the LED at a known current [13], [22]. The S and Q values for two group of commercial power LED models were extracted as reported in [15].

The technique can be applied also to a LED string; in such case, (5) can be expressed as:

$$V_F^* = n \cdot (S \cdot T^* + Q), \tag{6}$$

where n is the number of LEDs connected in series, V_F^* is the overall voltage of the series, and T^* is the average junction temperature of the devices.

Therefore, by imposing a precise probe current to the group of LEDs, and measuring the voltage drop at their terminals, it is possible to calculate the T^* from (6) once the proper S and Q values are chosen for the applied current.

III. LEDS DRIVING AND MEASUREMENT CIRCUIT

The measurement circuit is inspired by that presented in [15], based in turn on studies carried out on several junction devices [18], [22]. The new implementation makes the measurement fully compatible with existing driving circuits and allows to measure the average junction temperature of the LEDs in a string. In particular, it bypasses the needs of the fixed-current approach [14], [16], [18], [21], [22] by relying instead on the application of random currents I_{rnd}, which are however precisely measured in order to determine the correct $S(I_{rnd})$ and $Q(I_{rnd})$ values to be used in (5) or (6). The probe current is generated by properly setting the input parameters of the commercial LED driver ADP8140 [23], which is a 4-Channel driver with adaptable power control, able to sink an adjustable current from 125 µA to 500 mA for each channel. This highly integrated driver operates from 3 V to 30 V, with LED anode supply voltages up to 100 V. The maximum current is set by an external resistor R_{SET}, according to the equation:

$$R_{SET} = \frac{2560}{I_{SINK}}. \tag{7}$$

We set R_{SET} = 7.32 kΩ so that, by combining two current sink channels, up to 700 mA are delivered. The driver regulates the voltage at the LEDs anode by controlling a PMOS transistor. It also allows to dim the LED current down to very low values, through an analog or pulsed voltage control. In particular, an analog voltage between 0 V and 2 V linearly scales down the output current.

The driving and measurement circuit is described by the block scheme in Fig. 1. The LED string, composed of 5 white light power LED [24], is connected between the PMOS drain and the LED driver sink pins. A resistor of 100 mΩ is placed in series with the cathode to measure the LED current. A current sense amplifier (Texas Instrument INA285 [25]) with a gain of 1000 V/V is used to read the current, while two voltage dividers scale the anode and cathode voltages with a factor of 0.067 V/V. Finally, a microcontroller reads the LEDs voltages and currents, controls the driver dimming, and implements the measurement technique.

The microcontroller is a SAM C21, 32-bit ARM Cortex-M0+ [26], mounted on SAMC21 XplainedPro board

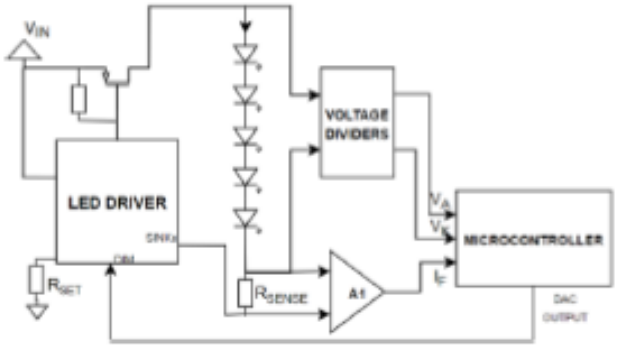

Fig. 1. Block scheme of the circuit.

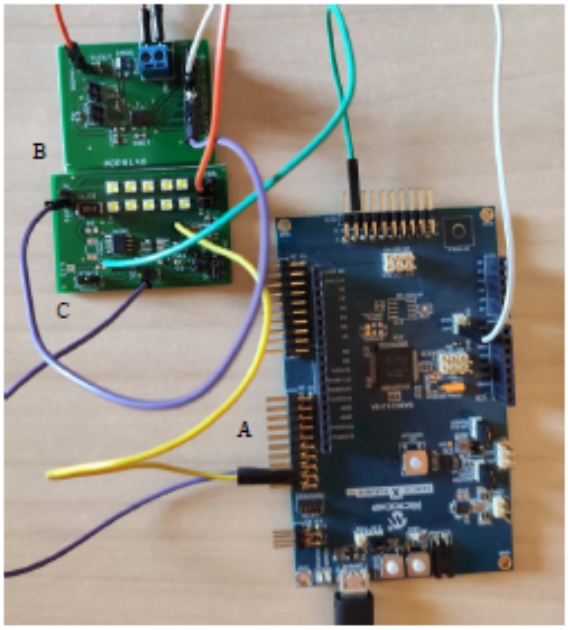

Fig. 2. Picture of the LEDs driving and measurement circuit, comprising the microcontroller development board (A), the ADP8140 LED driver (B), and the LEDs string board (C) which also includes the analog front-end for measurement of the string voltage and current.

[27]. It offers helpful features for the measurement technique, in particular up to two 12-bit and one 16-bit Analog-to-Digital Converters (ADCs), and a 10-bit Digital-to-Analog Converter (DAC). One 12-bit ADC is used to read the LED current, whereas the 16-bit differential ADC is used to read the overall LED series voltage. The DAC is used to impose and regulate the analog voltage to the LED driver dimming input. The use of low-power microcontroller and components, makes the additional energy consumption of the measurement circuit negligible compared to the energy required to power the LEDs.

Fig. 2 shows a picture of the development board, the driver, and the LED string. The same circuit can be obviously used for the monitoring of just one LED. Measuring instead the temperature of each single device is also possible, but requires a multiple-input ADC and a proper redesign of the PCB.

The microcontroller routine consists of two phases: the LED string normal working phase and the temperature-sensing phase. During the former phase, the LED current is set

at about 700 mA, imposing a suitable analog voltage to the dimming pin of the driver through the DAC peripheral. The temperature-sensing phase starts every 5 seconds, by setting the DAC to the lowest value, which allows to flow a fixed current through the LED of about 2 mA. Therefore, the LEDs stay in fact off for a few milliseconds, during the voltage and current acquisition and conversion time (about 1.4 ms). Then, the LED is turned back on, in this way there is no significant impact on the brightness of the LEDs. At each step, the DAC output is modified to impose a new current (I_{md}), anyhow in the range 2-10 mA. Measured currents and corresponding voltages are stored in two arrays in the microcontroller. Afterwards, $S(I_{md})$ and $Q(I_{md})$ are extracted, at the measured I_{md} , from the linear interpolations of the S and Q data taken from [15], and finally the average junction temperature of the LEDs in the string is calculated from (6).

IV. Results

The characteristics of the measurement circuit described in the previous section were assessed by performing several tests. The investigation was performed by heating the devices in a temperature-controlled oven. To prevent self-heating effects, the characterization tests were made by running only the temperature-sensing phase at low currents while disabling the normal working phase when the LEDs are fully on. The actual LED temperature was measured through a 1.1 °C accuracy thermocouple, placed in tight contact with the LEDs board. At each temperature increase, a sufficiently long time delay is waited in order to get the devices stabilize at the oven temperature. This way, we can be sure that the PCB and the junctions are in isothermal condition.

The temperatures estimated by the circuit were compared with the actual temperatures. Fig. 3 shows the error occurring in the T_J measurement at various actual temperatures. In order to assess the repeatability of the technique, several current-voltage acquisitions and up to ten T_J extractions were repeated at each set-up temperature, with random probe currents in the range from 2 mA to 10 mA. The corresponding values are shown in the graph with different colors.

The grey line is a guide-to-the-eye representing the average error. The overall average absolute error is 1.7 °C with a maximum error of 3.0 °C at 135 °C, and a maximum standard deviation of 0.5 °C; the peak-to-peak error is 4.9 °C. Several error sources contribute to this error, including sensor accuracy, measured current and voltage accuracy, noise, and how well the interpolated values of S and Q represent the LEDs in the string.

V. Conclusion

A circuit for measuring the junction temperature of a string of power LEDs used for solid-state lighting in luminaire platforms is presented. The circuit uses an off-the-shelf LED driver that can be found in commercial platforms. The measurement technique is based on the linear relationship between the junction temperature and voltage drop at a certain current value. The V-T_J relationship, which is predetermined and valid for all the LEDs with the same part number, is used by the microcontroller to calculate the average junction temperature of the LEDs in the string.

Experimental tests on samples of a commercial high-power LEDs show an absolute error below 3 °C for the typical temperature working range. The measurement routine takes few milliseconds and does not affect the normal operation of the LEDs.

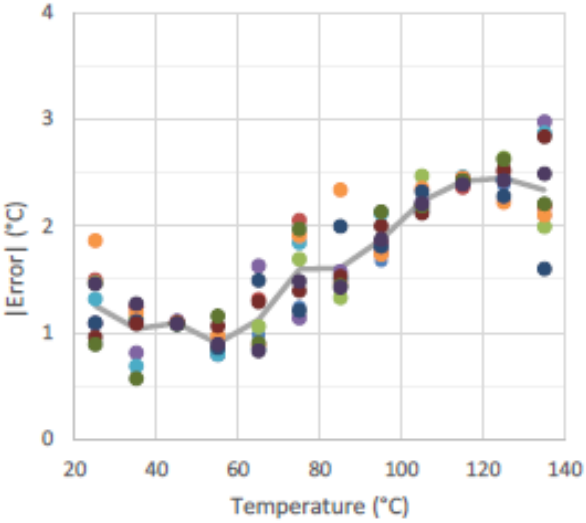

Fig. 3. Junction temperature measurement error for the LED string at ten different measurement routines; the continuous line is a guide-to-the-eye of the average error calculated over all the algorithm executions.

Acknowledgment

D. I. Author gratefully acknowledges *PAC Calabria 2014-2020 Asse Prioritario 12, Azione 10.5.12*.

References

[1] M.-H. Kim et al., "Origin of efficiency droop in GaN-based light-emitting diodes," Appl. Phys. Lett., vol. 91, no. 18, p. 183507, Oct. 2007.

[2] N. Narendran and Y. Gu, "Life of LED-Based White Light Sources," J. Disp. Technol., vol. 1, no. 1, pp. 167–171, Sep. 2005.

[3] M. Meneghini, M. Dal Lago, N. Trivellin, G. Meneghesso, and E. Zanoni, "Degradation Mechanisms of High-Power LEDs for Lighting Applications: An Overview," IEEE Trans. Ind. Appl., vol. 50, no. 1, pp. 78–85, Jan. 2014.

[4] F. K. Wang and T. P. Chu, "Lifetime predictions of LED-based light bars by accelerated degradation test," Microelectron. Reliab., vol. 52, no. 7, pp. 1332–1336, 2012.

[5] D. Iero, F. G. Della Corte, G. Fiorentino, and P. M. Sarro, "A calorimetry-based measurement apparatus for switching losses in high power electronic devices," in 2016 IEEE International Energy Conference (ENERGYCON), 2016.

[6] Z. Vaitonis, P. Vitta, and A. Žukauskas, "Measurement of the junction temperature in high-power light-emitting diodes from the high-energy wing of the electroluminescence band," J. Appl. Phys., vol. 103, no. 9, p. 093110, May 2008.

[7] C. C. Lee and J. Park, "Temperature Measurement of Visible Light-Emitting Diodes Using Nematic Liquid Crystal Thermography With Laser Illumination," IEEE Photonics Technol. Lett., vol. 16, no. 7, pp. 1706–1708, Jul. 2004.

[8] M. Horiuchi, Y. Yamagata, S. Tsutsumi, K. Tomita, and Y. Manabe, "Development of junction temperature estimation system for light-emitting LED using pulsed-laser Raman scattering," J. Solid State Light., vol. 2, no. 1, p. 7, Dec. 2015.

[9] Q. Chen, X. Luo, S. Zhou, and S. Liu, "Dynamic junction temperature measurement for high power light emitting diodes," Rev. Sci. Instrum., vol. 82, no. 8, 2011.

[10] JEDEC Solid State Technology Association, "Overview of Methodologies for the Thermal Measurement of Single- and Multi-Chip, Single- and Multi-PN- Junction Light-Emitting Diodes (LEDs) - JESD51-50," JEDEC Standards, no. April. Arlington, VA, 2012.

[11] JEDEC Solid State Technology Association, "Implementation of the Electrical Test Method for the Measurement of Real Thermal Resistance and Impedance of Light-Emitting Diodes with Exposed Cooling - JEDEC 51-51," JEDEC Standard, no. April. Arlington, VA, 2012.

[12] B. Wu et al., "Junction-temperature determination in InGaN light-emitting diodes using reverse current method," IEEE Trans. Electron Devices, vol. 60, no. 1, pp. 241–245, Jan. 2013.

[13] Y. Xi and E. F. Schubert, "Junction–temperature measurement in GaN ultraviolet light-emitting diodes using diode forward voltage method," Appl. Phys. Lett., vol. 85, no. 12, pp. 2163–2165, Sep. 2004.

[14] F. D. Roscam Abbing and M. A. P. Pertijs, "Light-emitting diode junction-temperature sensing using differential voltage/current measurements," in Proceedings of IEEE Sensors, 2011, pp. 861–864.

[15] F. Della Corte, G. Pangallo, R. Carotenuto, D. Iero, G. Marra, M. Merenda, and S. Rao, "Temperature Sensing Characteristics and Long Term Stability of Power LEDs Used for Voltage vs. Junction Temperature Measurements and Related Procedure," IEEE Access, vol. 8, pp. 43057–43066, 2020.

[16] S. Santra, P. K. Guha, S. Z. Ali, I. Haneef, and F. Udrea, "Silicon on Insulator Diode Temperature Sensor– A Detailed Analysis for Ultra-High Temperature Operation," IEEE Sens. J., vol. 10, no. 5, pp. 997–1003, May 2010.

[17] Y. B. Acharya and P. D. Vyavahare, "Study on the temperature sensing capability of a light-emitting diode," Rev. Sci. Instrum., vol. 68, no. 12, pp. 4465–4467, Dec. 1997.

[18] G. Brezeanu et al., "4H-SiC Schottky diodes for temperature sensing applications in harsh environments," in Materials Science Forum, 2011, vol. 679–680, pp. 575–578.

[19] F. G. Della Corte, G. Pangallo, S. Rao, R. Carotenuto, D. Iero, M. Merenda, and F. Pezzimenti, "Use of 4H-SiC-based diodes as temperature sensors," in Proceedings of the International Semiconductor Conference, CAS, 2019, pp. 71–74.

[20] S. Rao, L. Di Benedetto, G. Pangallo, A. Rubino, S. Bellone, and F. G. Della Corte, "85-440 K Temperature Sensor Based on a 4H-SiC Schottky Diode," IEEE Sens. J., vol. 16, no. 17, pp. 6537–6542, 2016.

[21] I. Josan et al., "Extreme environment temperature sensor based on silicon carbide schottky diode," in Proceedings of the International Semiconductor Conference, CAS, 2009, vol. 2, pp. 525–528.

[22] G. Pangallo, R. Carotenuto, D. Iero, E. D. Mallemace, M. Merenda, S. Rao, and F. G. Della Corte, "A Direct Junction Temperature Measurement Technique for Power LEDs," in 9th IEEE International Workshop on Applied Measurements for Power Systems, AMPS 2018 - Proceedings, 2018, vol. 1, no. 1, pp. 1–5.

[23] Analog Devices, "ADP8140 Datasheet," 2018. [Online]. Available: https://www.analog.com/media/en/technical-documentation/data-sheets/ADP8140.pdf. [Accessed: 30-Jun-2020].

[24] OSRAM Opto Semiconductors, "OSLON® Square LUW CQAR (streetwhite)," 2018. [Online]. Available: https://dammedia.osram.info/media/resource/hires/osram-dam-5537536/LUW CQAR (streetwhite)_EN.pdf.

[25] Texas Instruments Inc., "INA28x Datasheet," 2012. [Online]. Available: http://www.ti.com/lit/ds/symlink/ina283.pdf.

[26] Microchip Technology Inc., "SAM C20/C21 Family DataSheet," 2020. [Online]. Available: http://ww1.microchip.com/downloads/en/DeviceDoc/SAM-C20C21-Family-Data-Sheet-DS60001479E.pdf. [Accessed: 30-Jun-2020].

[27] Microchip Technology Inc., "SAM C21 Xplained Pro User Guide," 2016. [Online]. Available: http://ww1.microchip.com/downloads/en/devicedoc/Atmel-42460-SAM-C21-Xplained-Pro_User-Guide.pdf. [Accessed: 30-Jun-2020].

This is the post-print of the following article:

Proceedings of IEEE Sensors, 2020, 2020-October, 9278526.

Article has been published in final form at:

https://ieeexplore.ieee.org/document/9278526

DOI: 10.1109/SENSORS47125.2020.9278526

© 20xx IEEE. Personal use of this material is permitted. Permission from IEEE must be obtained for all other uses, in any current or future media, including reprinting/republishing this material for advertising or promotional purposes, creating new collective works, for resale or redistribution to servers or lists, or reuse of any copyrighted component of this work in other works.